EFFICIENCY OF CO_2 FOAM MOBILITY CONTROL WITH HETEROGENEOUS RESERVOIR PROPERTIES

Alv-Arne Grimstad[1*], Øystein Strengehagen Klemetsdal[2]
[1] SINTEF Industry, Postboks 4763 Torgarden, NO-7465 Trondheim, Norway
[2] SINTEF Digital, Postboks 124 Blindern, 0341 Oslo, Norway

* Corresponding author e-mail: alv-arne.grimstad@sintef.no

Abstract

We investigate how reservoir heterogeneity affects the efficiency of CO_2 mobility control in saline aquifer storage. An ensemble of reservoir models is set up for simulation of CO_2 injection with a quarter-five-spot well pattern where CO_2 is injected, and brine is produced for pressure control at opposite corners. Results with and without mobility control are compared. Additionally, results are generated for a modified foam model where the mobility reduction factor scales with reservoir permeability. An empirical foam model with partitioning of surfactant between the CO_2 and brine phases is used.

Keywords: CO_2 storage, CO_2 mobility control, CO_2-brine foam.

1. Introduction

Previous work has demonstrated that mobility control in saline aquifer storage of CO_2 can significantly increase storage efficiency [1]. The reservoir model in [1] had homogeneous permeability and porosity and was used to investigate the efficiency of mobility control for various combinations of mobility reduction factor, surfactant concentration and size of surfactant solution slug. Both CO_2-soluble and water-soluble surfactant was considered. The results showed that injection of a foam-stabilising surfactant solution in the first years of a CO_2 storage operation can significantly improve the storage efficiency, predominantly close to the injection well, and thereby delay the break-through time of CO_2 at wells used for pressure control by formation brine production.

In the present work the reservoir properties are not homogeneous, but randomly generated using a gaussian variogram. An ensemble with different realizations of the permeability and porosity is used to obtain statistics on the difference between foam effect in homogeneous and heterogeneous formations. Foam properties such as mobility reduction factor and partition coefficient are kept fixed in all simulations. This enables an investigation of the effect of reservoir heterogeneities on the efficiency of mobility control for CO_2 storage. Reservoirs with heterogeneous permeability and porosity may contain high-permeability streaks between injection and production wells, leading to significantly reduced storage capacity, since breakthrough of injected CO_2 at a pressure control well would necessitate shutting this well down. Pressure management in the storage reservoir would then be much reduced and rising pressure in the reservoir would rapidly diminish attainable injection rates.

Experiments with foam in porous media have indicated that contrasts in the mobility of injected gas can be smoothened out with use of foam [2][3]. The experiments also indicate that the mobility reduction factor for foam increase with increasing permeability. This smoothing effect would give an additional improvement to storage efficiency in heterogeneous reservoirs.

2. Method

We consider a geological model spanning a volume of 1400×1400×100 m, discretized by a 30×30×20 Cartesian grid. The top of the model is set to 800 m depth, with zero dip. To capture the propagating CO_2 front more accurately, the top six grid cell layers have a vertical thickness of 1.67 m. Vertical cell thickness increases linearly from layer six to the bottom, and the bottom six layers have a thickness of 8.33 m. CO_2 is injected through an injection well that perforates the bottom four layers in one corner of the model, at a constant injection rate of 366 000 m^3/day at surface conditions (equivalent to 250 kt/year), constrained at a maximum bottom-hole pressure of 150 bar. A brine production well perforates the bottom four layers in the opposite corner and is set to operate at a constant bottom-hole pressure of 90 bar.

Both brine and CO_2 relative permeabilities are represented by Corey-type curves with exponent 2. Residual saturations are set to 0.3 for CO_2 and 0.2 for brine. Capillary entry pressure for CO_2 in the storage formation is set to 0.15 bar. All boundary conditions for the model (except for the wells) are set to no-flow.

We simulate injection of CO_2 first for four years with timesteps starting at 0.35 days, and gradually increasing to 90 days. During this period, we also inject surfactant dissolved in the CO_2 stream at 1% wt. The surfactant is assumed to have a partition coefficient of 1.0, meaning that at equilibrium where both brine, CO_2 and surfactant are present in the reservoir the mass concentration of surfactant in brine and CO_2 will be equal. We assume that the surfactant works to stabilise CO_2-brine foam wherever the surfactant concentration is large enough. The empirical foam model of Vassenden and Holt [5] is

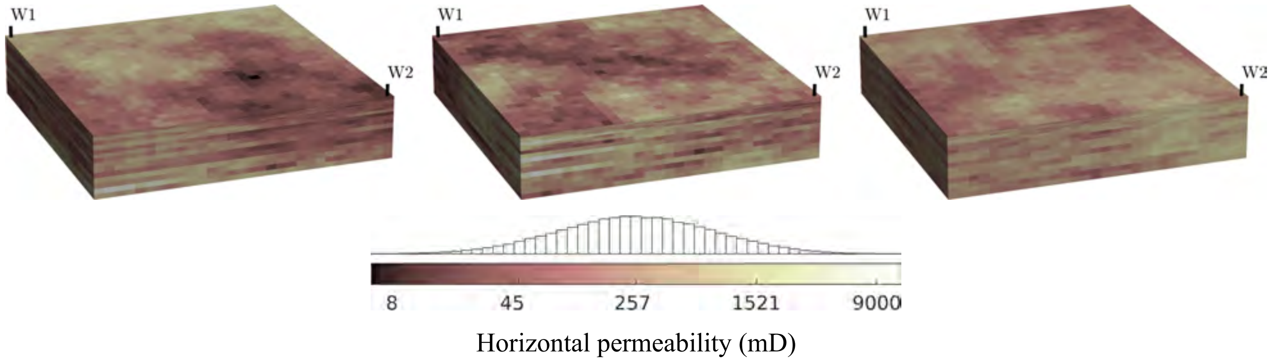

Figure 1. Horizontal permeability for the first three realizations of the ensemble. The histogram reports the horizontal permeability distribution of the entire ensemble.

used to describe the effect the foam has on the CO_2 relative permeability, modified with a concentration term as discussed in [1]. A mobility reduction factor of 10 is used. After the initial period of co-injection of surfactant and CO_2, we continue injection of pure CO_2 until breakthrough in the production well, using timesteps of 180 days. To compare the effect of using surfactant for mobility control, we also simulate the same setup without surfactant injection during the first four years.

All simulations are done using a dedicated CO_2 foam model developed in the MATLAB Reservoir Simulation Toolbox (MRST) [4]. The governing equations describing conservation of water, gas and surfactant masses, are discretized using finite-volumes with single-point upwind weighting in space, and implicit, backward Euler time stepping.

To construct an ensemble of heterogeneous geomodels, we use the newly developed ensemble module in MRST. We generate an ensemble of 100 permeability/porosity realizations by means of a stationary Gaussian process on the $[0,1]^3$ cube [6], repeated four times to create a horizontally layered structure often seen in geomodels. Permeabilities are lognormal, whereas porosities are normal, both generated from the same Gaussian process:

$$\log_{10}(K) = N(-12.5, 0.5), \phi = N(0.25, 0.5) \quad (1)$$

(Permeability in units of m^2. K_v/K_h=1/10.) Figure 1 shows the permeability distribution for the first three realizations, along with a histogram for the entire ensemble. The MRST ensemble module allows us to simulate batches of realizations in parallel using background MATLAB sessions, which significantly reduces the total simulation time.

To explore the idea of a permeability-dependent foam strength we also run the ensemble with the mobility reduction factor modified by a permeability dependent factor

$$P(K) = (K/K_{\text{ref}})^2 \quad (2)$$

where the horizontal permeability is used for the evaluation, and K_{ref} is set to $\exp\left(\overline{\ln(K)}\right)$, i.e., the exponential of the logarithmic mean of the permeability in the ensemble (about 260 mD).

3. Results

In the following, we present results for three different types of simulations using the 100-realization ensemble: pure CO_2 injection; CO_2 injection using foam with mobility reduction factor independent of permeability; and CO_2 injection using foam with mobility reduction factor dependent on permeability according to Eq. (2). In the following, we refer to these as 'no foam', 'foam', and 'p-foam', respectively. We compare the two ensemble simulations using foam to no foam and to each other, and also accompany the results with a set of simulations with homogeneous permeability and porosity of 260 mD and 0.25, respectively.

3.1. *Foam vs no foam*

Figure 2 and Figure 3 show the results from the ensemble simulations with foam, compared to simulations without foam. Figure 2 shows a histogram of relative increase in storage efficiency for the same porosity/permeability realizations. Storage efficiency is in each case calculated as the fraction of pore volume occupied by CO_2 at the time of CO_2 breakthrough in the pressure control well.

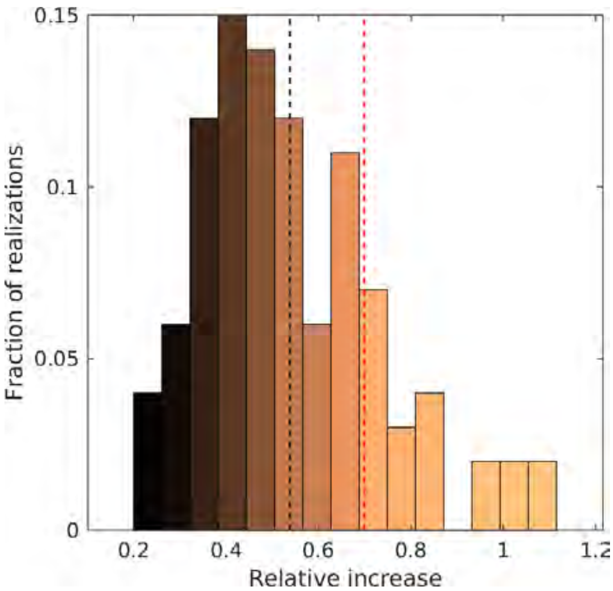

Figure 2. Histogram of relative increase in stored CO_2 mass by using foam. The mean is indicated by a black, dashed line, and the red, dashed line shows the relative increase for the same simulations using homogeneous permeability/porosity. The bars are coloured by the corresponding relative increase.

We see that the storage efficiency increases in all realizations, and range from 20 % increase to about 110 % increase, with average increase about 54 %, indicated by the black vertical dashed line in the figure. Results from the simulation on a homogeneous model, an increase of 70 % is indicated by the red vertical dashed line. Figure 3 shows a correlation plot of the storage efficiency for each ensemble realization with and without foam. The storage efficiency without foam ranges mainly from 12 to 22 %, with an outlier at 24 %. With foam the storage efficiency ranges from 21 to 39 %, with an outlier at 42 %.

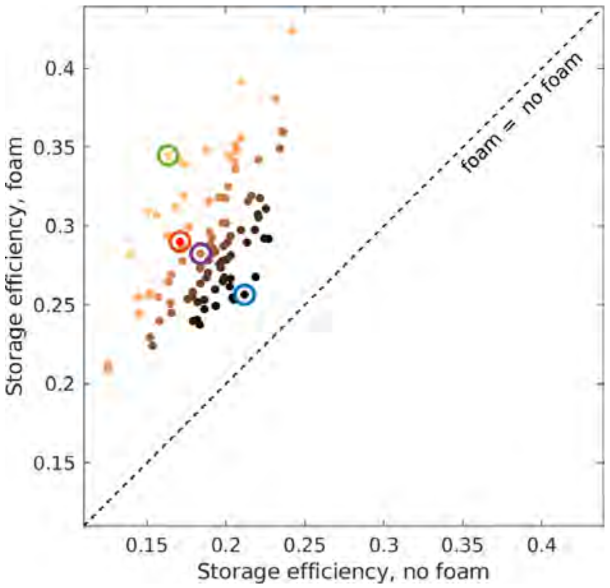

Figure 3. Correlation plot reporting storage efficiency (in pore volume fraction) using foam vs. no foam. The dashed line corresponds to zero gain, and the red dot represents the simulation with homogeneous rock properties.

In the correlation plot the three ensemble realizations with smallest, largest and an intermediate increase in storage efficiency are marked with blue, green and purple circles. These same ensemble realizations are marked similarly in the other correlation plots later. In addition, the result for the model with homogeneous porosity and permeability is marked with a red circle.

3.2. P-foam vs no foam

Figure 4 and Figure 5 show the results from the simulations with p-foam, compared to simulations without foam. The relative increase in storage efficiency (Figure 4) is now larger and range from 50 to 335 %, with an average value of 138 %. For the homogeneous model, the relative increase in storage efficiency is 70 %, the same as for normal foam vs no foam. This is as expected, since the foam strength in the homogeneous case will be the same for both normal foam and p-foam with the scaling given in Eq. (2). For the heterogeneous models, the foam strength scaling will cause reduced flow in the high-permeable regions compared to normal foam, and an increased sweep of low-permeable areas close to the injection well, thereby increasing the amount of stored CO_2.

The correlation plot (Figure 5) shows that the range of storage efficiency is shifted to 29 to 57 % for the p-foam cases. It also shows that other realizations than for ordinary foam score highest and lowest in storage efficiency increase.

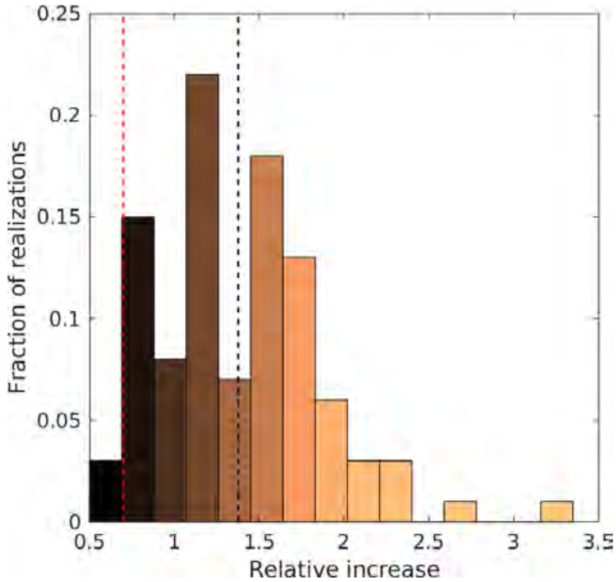

Figure 4. Histogram of relative increase in stored CO_2 mass by using p-foam compared to no foam. The mean is indicated by a black, dashed line, and the red, dashed line shows the relative increase for the same simulations using homogeneous permeability/porosity.

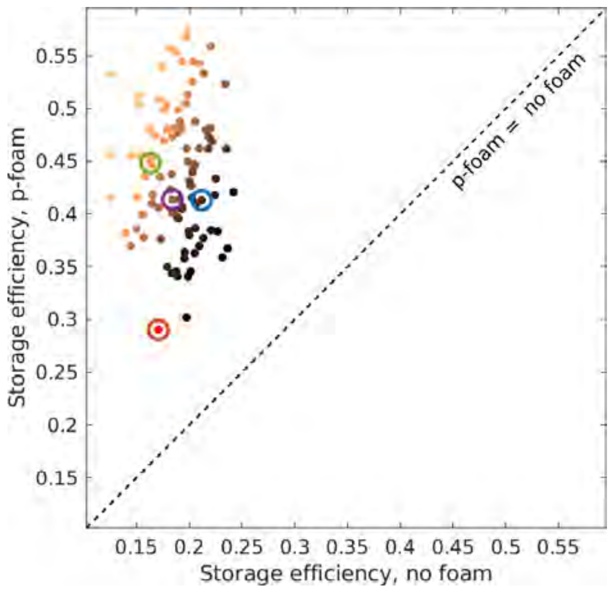

Figure 5. Correlation plot reporting storage efficiency (in pore volume fraction) using p-foam vs. no foam. The dashed line corresponds to zero gain, and the red dot the simulation with homogeneous rock properties.

3.3. Foam vs p-foam

Finally, Figure 6 and Figure 7 show a comparison of the results from p-foam simulations with the simulations using normal foam. We see that most realizations see an increase in the amount of stored CO_2, some as high as 150 %. However, for a few realizations the increase is only minor, and two realizations even see a small reduction in the amount of stored CO_2 for p-foam simulations (Figure 7). The mean increase is 56 %.

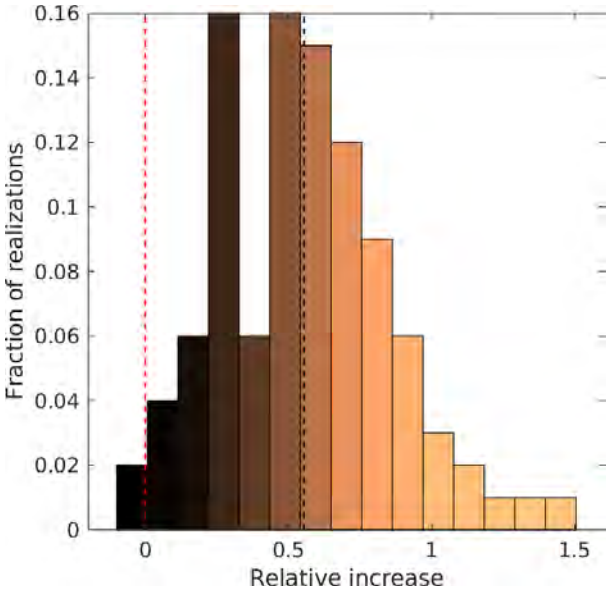

Figure 6. Histogram of relative increase in stored CO_2 mass by using p-foam, compared to normal foam. The mean is indicated by a black, dashed line, and the red, dashed line shows the relative increase for the same simulations using homogeneous permeability/porosity.

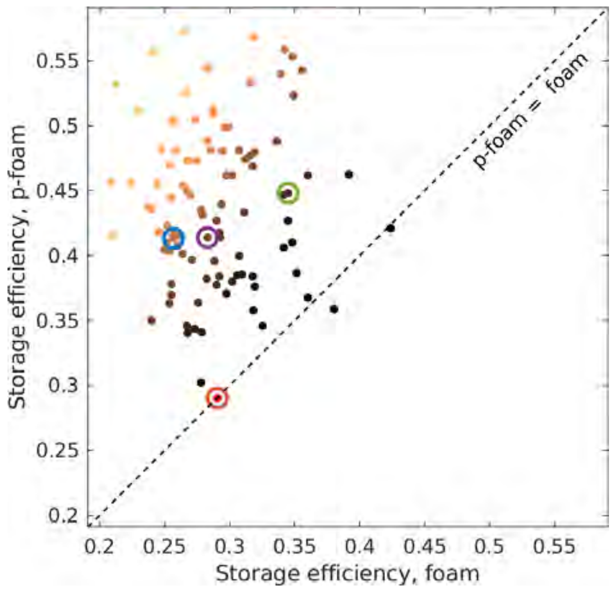

Figure 7. Correlation plot reporting storage efficiency (in pore volume fraction) using p-foam vs. normal foam. The dashed line corresponds to zero gain, and the red dot the simulation with homogeneous rock properties.

3.4. Distribution of injected CO_2

The distribution of injected CO_2 at breakthrough is illustrated in Figure 8 for a selection of realisations and foam properties. For this figure the CO_2 saturation at the end of the simulations (at break-through) is pore-volume averaged in the vertical direction and the resulting values plotted with the position of the injection well in the lower left corner and the pressure control well in the upper right corner in each subplot (shown only in the upper left subplot). Simulations without foam are shown in the top row; simulations with normal foam in the middle row and

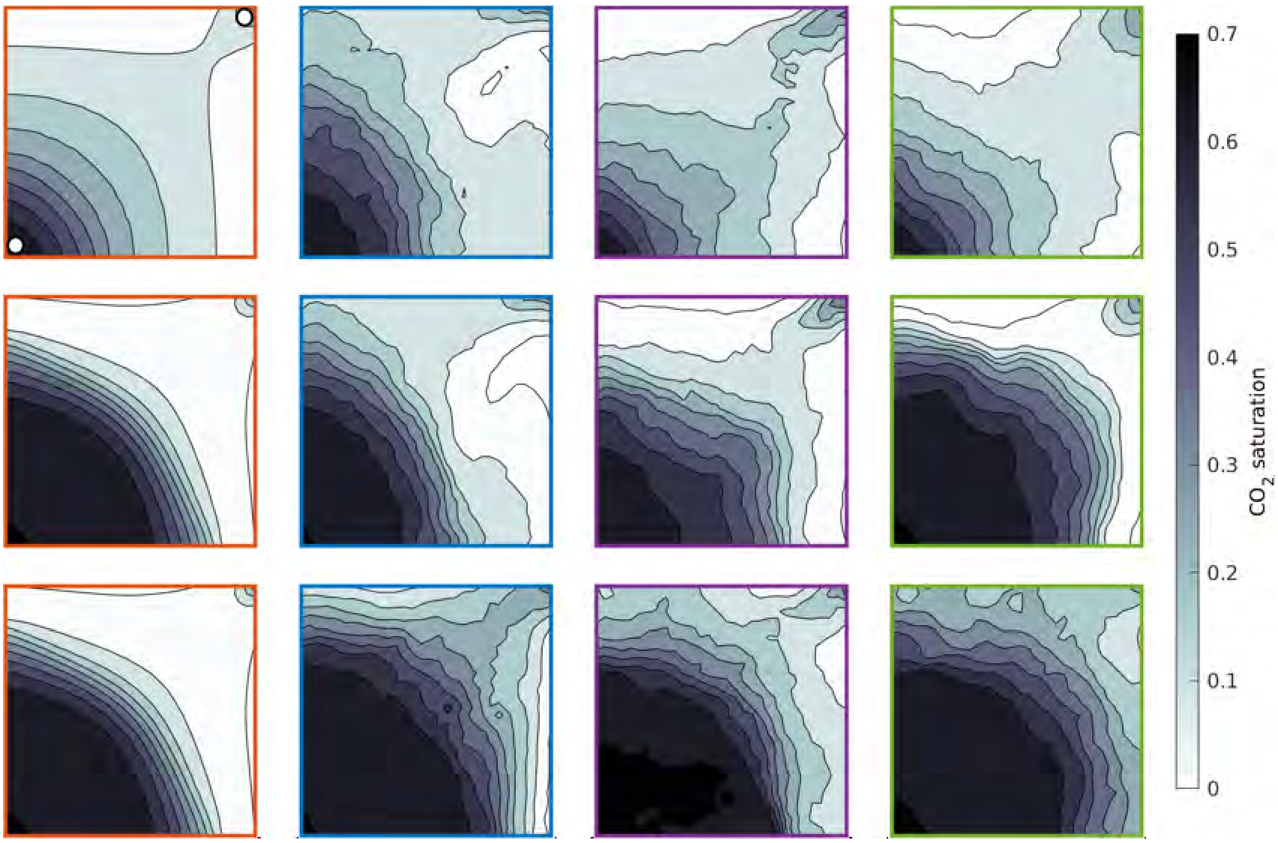

Figure 8. CO_2 plume for four selected cases. From top to bottom: no foam, foam, p-foam. From left to right: Homogeneous rock followed by the realizations with lowest gain, mean gain and largest gain from the ensemble simulation with foam vs no foam (Figure 3). The border colour of each subplot corresponds to the colour of the circles in the correlation plots in Figure 3, 5 and 7.

with p-foam in the bottom row. The columns, with different-coloured borders show results with the homogeneous model, and results from the realizations with lowest, mean and maximum storage efficiency increase in the foam vs no foam comparison (Figure 3). The colour of the border for each subplot corresponds to the models with similarly coloured markers in Figure 3, 5 and 7.

It is seen that, as expected, simulations with high storage efficiency have high average CO_2 saturations in a large region out from the injection well. We note that the transition from high to low saturation is sharper in the foam cases than in the no-foam case, indicating a more piston-like displacement of brine by the injected CO_2 even for the relatively high density difference between CO_2 and brine. We also note a tendency for more circular shape of the high-saturation CO_2 plume in the p-foam cases than for the normal foam and no-foam cases, indicating that the effect of heterogeneities on the shape of the CO_2 plume is diminished for the p-foam simulations. Figure 9 shows CO_2 saturation pore-volume averaged along the x axis for the same realizations as in Figure 8 at the time of CO_2 breakthrough in the pressure control well. The perforations in the injection and pressure control wells are indicated in the upper left subplot. We observe that the CO_2-plume is thicker for the foam cases (second and third row) and thickest for the p-foam case (third row), although the effect is only minor for the ordinary foam case with the least increase in storage efficiency (second subplot on the second row).

4. Discussion and conclusions

The BHP constraint imposed in the injection well cause throttling of the injection rate in most of the cases with foam and for all cases with p-foam, for part of the injection period. This can be expected, due to the larger pressure gradients in the near-well region when mobility control is used. Shear-thinning of foam, which is not included in the present simulations, would give weaker mobility reduction close to the injection well and thereby reduce the impact on injection rates. A reduced injection rate due to too high BHP would not be desirable in a storage project where a constant injection rate has been agreed upon in a contract with the owner of the CO_2 source. New simulations with shear-thinning included should be run to examine more closely the impact that can be expected on injection rates.

Simulation results presented here demonstrate that the storage efficiency can be significantly increased with mobility control both for homogeneous and heterogeneous reservoir properties. The relative increase in the amount of CO_2 injected at the time of break-through in the pressure control well range from 20 to 110 % simulations with permeability-independent foam strength (normal foam) and from 50 to 335 % for the simulations where the foam strength scales with the permeability (p-foam). The average relative increase in amount of stored CO_2 is 54 % for normal foam and 138 % for p-foam.

The results show, however, that the relative increase in stored amount from normal foam to p-foam for some members of the ensemble is quite small. In the limiting case of homogeneous permeability this is easily explained, since the foam strength for normal foam and p-foam in that case is by definition equal. For the heterogeneous cases the difference would depend on the shape of permeability/porosity patterns in the reservoir.

In our results, introducing permeability-dependent foam strength significantly increases storage efficiency compared to using normal foam. However, we emphasize that we have only considered a single type of permeability dependence in this work, and further investigations of different models are needed to draw firm conclusions. We also mention that introducing permeability dependence in the mobility reduction factor makes the setup significantly more challenging to simulate. For some of the ensemble members, this

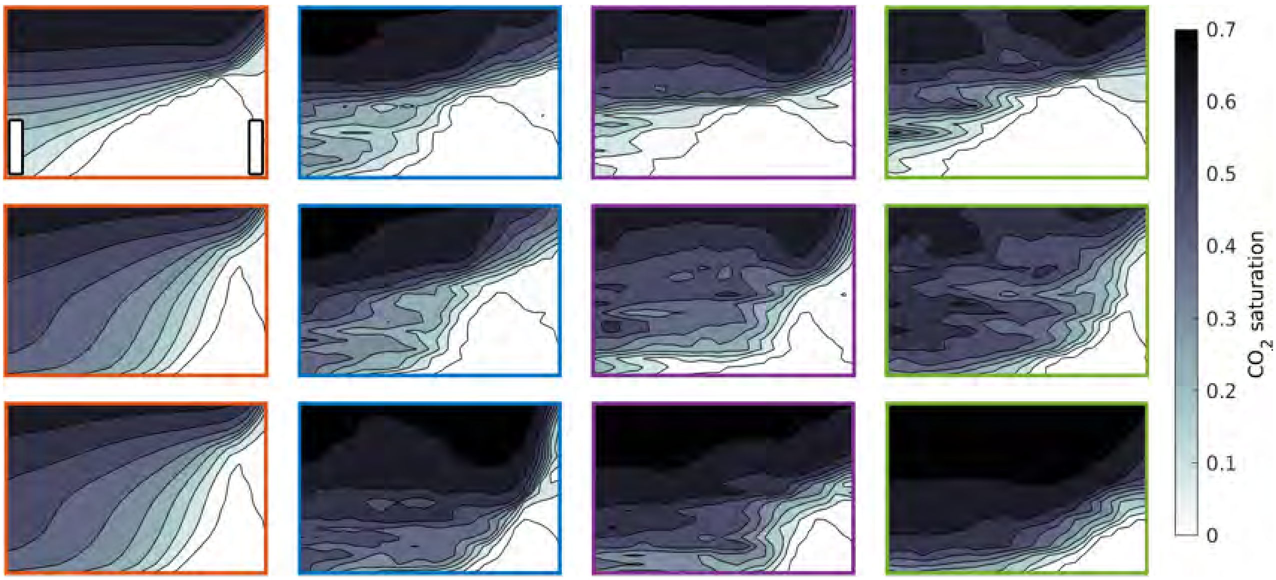

Figure 9. Vertical plot of the CO_2 saturation along the diagonal between injection and pressure control wells for selected cases. From top to bottom: no foam, foam, p-foam. From left to right: Homogeneous rock followed by the realizations with lowest gain, mean gain and largest gain from the ensemble simulations with foam vs no foam (Figure 3). The border colour of each subplot corresponds to the colour of the circles in the correlation plots in Figure 3, 5 and 7.

resulted in shorter timesteps and effectively less numerical diffusion for the p-foam ensemble. This may lead to an additional bias towards later breakthrough times compared to the no-foam and foam ensembles.

Acknowledgements

This publication has been produced with support from the NCCS Research Centre, performed under the Norwegian research program Centres for Environment-friendly Energy Research (FME). The authors acknowledge the following partners for their contributions: Aker Solutions, Ansaldo Energia, Baker Hughes, CoorsTek Membrane Sciences, EMGS, Equinor, Gassco, Krohne, Larvik Shipping, Lundin, Norcem, Norwegian Oil and Gas, Quad Geometrics, Total, Vår Energi, and the Research Council of Norway (257579/E20).

References

[1] Grimstad, A.-A., Bergmo, P., Nilsen, H.M., Klemetsdal, Ø. 2018. CO_2 storage with mobility control. GHGT-14, Melbourne, Australia.

[2] Chowdiah, P., Misra, B.R., Kilbane, J.J., Srivastava, V.J., Hayes, T.D. 1998, Foam propagation through soils for enhanced in-situ remediation. Journal of Hazardous Materials, 62 (3).

[3] Farajzadeh, R., Lotfollahi, M., Eftekhari, A.A., Rossen, W.R., Hirasaki, G.J.H. 2015. Effect of permeability on implicit-texture foam model parameters and the limiting capillary pressure. Energy & Fuels, 29 (5).

[4] Lie, K.-A. 2019. An introduction to reservoir simulation using MATLAB/GNU Octave: User guide for the MATLAB Reservoir Simulation Toolbox (MRST). Cambridge: Cambridge University Press. Doi:10.1017/9781108591416.

[5] Vassenden, F., Holt, T. 2000. Experimental foundation for relative permeability modelling of foam. SPE Reservoir Evaluation and Engineering, 3 (2).

[6] Wood, A., Chan, G. 1994. Simulation of Stationary Gaussian Processes in $[0, 1]^d$. Journal of Computational and Graphical Statistics, 3 (4).